

# Journal Pre-proof

Circulating exosomal microRNAs and subclinical atherosclerosis in obstructive sleep apnea

David Sanz-Rubio Inmaculada Martín-Burriel Jorge Rodríguez  
Marta Marín-Oto Abdelnaby Khalyfa Manuel Sánchez-de-la-Torre  
David Gozal Jose M. Marin



PII: S0300-2896(24)00477-0

DOI: <https://doi.org/doi:10.1016/j.arbres.2024.12.005>

Reference: ARBRES 3708

To appear in: *Archivos de Bronconeumología*

Received Date: 19 September 2024

Accepted Date: 12 December 2024

Please cite this article as: Sanz-Rubio D, Martín-Burriel I, Rodríguez J, Marín-Oto M, Khalyfa A, Sánchez-de-la-Torre M, Gozal D, Marin JM, Circulating exosomal microRNAs and subclinical atherosclerosis in obstructive sleep apnea, *Archivos de Bronconeumología* (2024), doi: <https://doi.org/10.1016/j.arbres.2024.12.005>

This is a PDF file of an article that has undergone enhancements after acceptance, such as the addition of a cover page and metadata, and formatting for readability, but it is not yet the definitive version of record. This version will undergo additional copyediting, typesetting and review before it is published in its final form, but we are providing this version to give early visibility of the article. Please note that, during the production process, errors may be discovered which could affect the content, and all legal disclaimers that apply to the journal pertain.

© 2024 Published by Elsevier España, S.L.U. on behalf of SEPAR.

## SCIENTIFIC LETTER

Circulating exosomal microRNAs and subclinical  
atherosclerosis in obstructive sleep apnea

David Sanz-Rubio <sup>1</sup>, Inmaculada Martín-Burriel <sup>2,3</sup>, Jorge Rodríguez <sup>1</sup>, Marta Marín-Oto <sup>1</sup>, Abdelnaby Khalyfa <sup>4</sup>, Manuel Sánchez-de-la-Torre <sup>6,7</sup>, David Gozal <sup>5</sup>, Jose M. Marin <sup>1,7,8</sup>

<sup>1</sup> Precision Medicine in Respiratory Diseases Group, Hospital Universitario Miguel Servet, Instituto de Investigación Sanitaria de Aragón (IIS Aragón), 50009 Zaragoza, Spain; [davidsanzrubio91@gmail.com](mailto:davidsanzrubio91@gmail.com) (D.S.-R.); [jrsanz265@gmail.com](mailto:jrsanz265@gmail.com) (J.R.-S.); [martamarinoto@gmail.com](mailto:martamarinoto@gmail.com) (M.M.-O.); [jmmarint@unizar.es](mailto:jmmarint@unizar.es) (J.M.M)

<sup>2</sup> Laboratorio de Genética Bioquímica (LAGENBIO), Instituto Agroalimentario de Aragón IA2 (UNIZAR-CITA), Instituto de Investigación Sanitaria de Aragón (IIS Aragón), Universidad de Zaragoza, 50013 Zaragoza, Spain; [minma@unizar.es](mailto:minma@unizar.es) (I.M.-B)

<sup>3</sup> Centro de Investigación Biomédica en Red de Enfermedades Neurodegenerativas (CIBERNed), Madrid, Spain

<sup>4</sup> Departments of Biomedical Sciences and <sup>5</sup> Pediatrics, Joan C. Edwards School of Medicine, Marshall University, Huntington, WV 25701, USA

<sup>6</sup> Group of Precision Medicine in Chronic Diseases, Hospital Nacional de Paraplégicos. IDISCAM. Department of Nursing, Physiotherapy and Occupational Therapy. Faculty of Physiotherapy and Nursing, University of Castilla-La Mancha, Toledo, Spain.

<sup>7</sup> Centro de Investigación Biomédica en Red de Enfermedades Respiratorias (CIBERes), Madrid, Spain

<sup>8</sup> Respiratory Service, Hospital Universitario Miguel Servet, University of Zaragoza, 50009 Zaragoza, Spain;

Corresponding author. David Sanz-Rubio, Precision Medicine in Respiratory Diseases Group, Hospital Universitario Miguel Servet, Instituto de Investigación Sanitaria de Aragón (IIS Aragón), 50009 Zaragoza, Spain. Email: [davidsanzrubio91@gmail.com](mailto:davidsanzrubio91@gmail.com)

Obstructive sleep apnea (OSA) is characterized by periodic collapse of the upper airway during sleep leading to intermittent hypoxia (IH) and arousals from sleep<sup>1</sup>. These events are associated with acute cardiometabolic changes and increased risk of cardiovascular disease and mortality<sup>2</sup>. Early development of subclinical atherosclerosis (SA) has been associated with OSA<sup>3</sup>. SA is defined as the presence of at least one atheroma plaque in the absence of any symptoms, being a risk factor by itself for developing cardiovascular events<sup>4</sup>. The mechanism by which OSA promotes early onset of SA is unknown.

Exosomes participate in cell-to-cell communication through their cargo, which includes microRNA (miRNA), proteins, or lipids<sup>5</sup>. Exosomes from children with OSA exhibited an altered miRNA cargo which promotes endothelial dysfunction<sup>6</sup>. Changes in the exosomal miRNA profile have also been reported in healthy young adults exposed to IH<sup>7</sup> and we showed that exosome from adults with OSA enhanced endothelial dysfunction in vitro<sup>8</sup>. Here, we compare eleven miRNAs (previously linked to SA, Table S1) in exosomes from patients with OSA and SA (OSA-SA), without SA and healthy control subjects. Participants were selected from the “Epigenetic Modifications in Obstructive Sleep Apnea Study” (EPIOSA) (NCT014575421), an ongoing long-term longitudinal cohort study at the Hospital Universitario Miguel Servet (Zaragoza, Spain)<sup>9</sup>. We followed current guidelines and regulations, the recommendations of the Declaration of Human Rights and the Conference of Helsinki. The experimental protocols were approved by the Instituto Investigación Sanitaria de Aragón Institutional Review Board (IRB #15/2013). All participants gave written informed consent. Home sleep tests were

conducted, and patients diagnosed with OSA received management based on current Spanish national guidelines. The carotid intima-media thickness (CIMT) measurement was performed using a Philips IU22 ultrasound system (Philips Healthcare, USA) with linear high-frequency 2-dimensional probes using the Bioimage Study protocol for carotid arteries. SA was defined as the presence of  $\geq 1$  atheromatous plaque, identified as a focal vessel wall thickness of  $\geq 1.5$  mm in any examined carotid artery. Fasting blood samples were taken and we followed our described methodology for exosome isolation and miRNA analysis<sup>10</sup>. Assessment of exosome integrity was performed by transmission electron microscopy, nanoparticle tracking analysis and dot blot (Fig. S1). Relative miRNA expression was determined using the  $\Delta\Delta\text{Ct}$  method.

At the exploratory study, we included 50 OSA patients (apnea-hypopnea index–AHI  $\geq 10$  events/hour sleep; e/h) and 16 age- and sex-matched healthy subjects (AHI  $\leq 10$  e/h) (Table S2). Three exosomal miRNAs were overexpressed in patients with OSA-SA (Fig. 1): miR-21-5p (relative expression, RE = 2.91), miR-145-5p (RE = 2.12) and miR-320a-3p (RE = 4.06). We evaluated the predictive potential of SA. The univariate ROC curve analysis displayed significant values for miR-21-5p ( $p = 0.0284$ ), miR-145-5p ( $p = 0.0072$ ) and miR-320a-3p ( $p = 0.0001$ ) but only miR-320a-3p (Fig. S2) showed potential to discriminate SA in OSA with a value of area under the curve (AUC) of 0.8125 (0.6834–0.9416). miR-320a-3p has been related to atherogenic progression in response to electrophilic stress response induced by oxidized phospholipids<sup>11</sup>, which is consistent with its increase in OSA-SA. In heart failure studies, miR-320a-3p was directly linked to an increase in all-cause mortality within 90 days of the event<sup>12</sup>. This finding could be related to the direct consequences of OSA on the cardiovascular system.

For validation, 50 OSA patients, 38 OSA-SA and 24 matched controls were selected. All subjects were also re-evaluated after 1 year, when OSA was divided into CPAP treated (n = 28) and those who refused CPAP treatment (n = 22). A similar partition was performed in the OSA-SA group, yielding 25 patients with and 13 without CPAP treatment. Blood pressures, ApoB, hsCRP and triglycerides were elevated in both OSA groups. At the 1-year follow-up period OSA patients irrespective of SA status also presented an increase in their CIMT values. Of note, OSA-SA NT patients showed a significant increase in ApoB, total cholesterol and LDL (Table S3). MiR-320a-3p recapitulated previous findings (RE = 2.66 among OSA-SA, AUC of 0.798) (Fig. 1). We also fitted miR-320a-3p to the multivariate logistic regression model including AHI and APO B (ROC analysis: AUC = 0.885;  $p < 0.0001$ ).

After 1 year of CPAP treatment, exosomal miR-320a-3p remained elevated in all groups of patients with OSA (Fig. 2). This was surprising considering that this miRNA has been linked to atherogenic progression through regulation of serum response factor<sup>13</sup> and response to electrophilic stress<sup>11</sup>. To reconcile these a priori contradictory findings, re-evaluation of CIMT at the 1-year follow-up allowed us to assess the predictive value of this miRNA as a marker of the progression of atherosclerosis. We found that higher levels of miR-320a-3p were related to a higher increase in CIMT from baseline ( $p = 0.0003$ ), and therefore a persistent higher cardiovascular risk (Fig. 2). Consequently, CPAP treatment that effectively corrects intermittent hypoxia, seems not enough to reverse the pathophysiological processes previously activated by the presence of OSA. The temporal changes in miR-320a-3p support the validity of this assumption. Notably, this hypothesis has been partially corroborated by animal studies. In a

mouse model of OSA, discontinuing intermittent hypoxia did not eliminate the pro-inflammatory activity of vascular wall macrophages. These cells exhibited epigenetic modifications in gene pathways associated with atherogenesis<sup>14</sup>. Similarly, in a murine model, "adherent treatment" for OSA failed to reverse many OSA-induced end-organ morbidities, likely involving senescence-related pathways<sup>15</sup>.

Target prediction and enrichment analyses of miR-320a-3p suggested an interesting role of this miRNA in the context of OSA-SA (Table S4-7). Alterations in cell adhesion have been linked to cell senescence and lately to the atherogenic process<sup>16</sup>. Additionally, OSA has been shown to accelerate biological aging<sup>17</sup>. T-cell metabolic disruptions have also been reported in OSA, which are associated with an increased incidence of various types of malignant tumors<sup>18</sup>. Pathway enrichment analysis revealed the involvement of the Wnt signaling pathway, previously linked to plasma exosomal miRNAs from OSA patients with reverse dipping blood pressure<sup>19</sup>. Furthermore, dysregulation of the cadherin pathway, particularly VE-cadherin, has been observed in OSA patients. This dysregulation may increase endothelial permeability, promote endothelial-to-mesenchymal transition, and ultimately contribute to atheroma plaque formation<sup>20</sup>.

This study has several limitations. First, this work evaluated a population with no comorbidities other than OSA avoiding confounding factors such as hypertension so, our findings cannot be applied to the general population. Second, we evaluated a restricted subset of exosomal miRNAs related to atherosclerosis. This selection could lead to underestimation of the role of exosomes. Future analyses will assess a broader and more comprehensive profile of miRNAs. Finally, our study describes alterations in the exosomal miRNA profile and does

not implicitly ascribe causality; however, further functional assays coupled to treatment and experimental models should contribute to further understanding on the roles of those miRNAs in OSA.

In summary, exosomal miRNAs are altered in the progression of atherogenic processes associated with OSA. Notably, the increased abundance of exosomal miR-320a-3p in OSA patients with SA was confirmed in two independent studies, thereby conferring validity to the potential use of this miRNA as a biomarker of SA in OSA. Finally, CPAP treatment did not reverse the altered levels of miR-320a-3p which suggests that CPAP may not be sufficient to reverse the atherosclerosis related pathways initiated and propagated by OSA.

#### Final declarations:

- Financial Disclosure: This research was funded by grants from Instituto de Salud Carlos III, Spanish Ministry of Health, Spain and the European Regional Development Fund (FEDER) (CD22/00033; PI21/01954, PI18/01524 and PI15/01441) and Department of Science and Universities, Government of Aragon, Spain (CUS/1466/2020; B22\_20R). DG is supported in part by National Institutes of Health grants HL166617 and HL169266. M.S-T. received financial support from a "Ramón y Cajal" grant (RYC2019-027831-I) from the "Ministerio de Ciencia e Innovación - Agencia Estatal de Investigación" cofunded by the European Social Fund (ESF)/"Investing in your future"

- Conflicts of interest: the authors declare not to have any conflicts of interest that may be considered to influence directly or indirectly the content of the manuscript
- Artificial intelligence involvement: None of the content was produced with the help of an artificial intelligence software or tool.
- Author contributions: Conceptualization, D.S-R., I.M-B., and J.M.M.; methodology, D.S-R., I.M.-B., J.R-S., A.K., and J.M.M.; investigation, D.S.-R., I.M-B, J.R-S., M.M-O., and J.M.M; patient recruitment, J.R-S., M.M-O., and J.M.M; data curation, D.S-R., J.R-S. and J.M.M; writing—original draft preparation, D.S.-R.; writing—review and editing, D.S.-R., I.M.-B, J.R-S., M.M-O., A.K., M.S-T., D.G. and J.M.M.; project coordination, D.S.-R.; and funding acquisition, D.S-R. and J.M.M. All authors have read and agreed to the submitted version of the manuscript.
- Acknowledgements: We are immensely grateful to the PRES group research team for their support in recruiting and following up with the patients. We appreciate the nurses' support at the Sleep Unit and Respiratory Department of the Hospital Universitario Miguel Servet in assisting with recruitment. The authors would like to acknowledge the use of Servicio General de Apoyo a la Investigación-SAI from the University of Zaragoza.

1. Heinzer, R. *et al.* Prevalence of sleep-disordered breathing in the general population: the HypnoLaus study. *Lancet Respir Med* 3, 310–318 (2015).
2. Marin, J. M., Carrizo, S. J., Vicente, E., Agusti, A. G. & Marin JM, C. S. *et al.* Long-term cardiovascular outcomes in men with obstructive sleep apnoea-hypopnoea with or without treatment with continuous positive airway pressure: an observational study. *Lancet* 365, 1046–1053 (2005).
3. Drager, L. F., Polotsky, V. Y. & Lorenzi-Filho, G. Obstructive Sleep Apnea. *Chest* 140, 534–542 (2011).
4. Baber, U. *et al.* Prevalence, Impact, and Predictive Value of Detecting Subclinical Coronary and Carotid Atherosclerosis in Asymptomatic Adults The Biolmage Study. *JACC* 65, 1065–1074 (2015).
5. Lässer, C. *et al.* Human saliva, plasma and breast milk exosomes contain RNA: uptake by macrophages. *J Transl Med* 9, 9 (2011).
6. Khalyfa, A. *et al.* Circulating Plasma Extracellular Microvesicle MicroRNA Cargo and Endothelial Dysfunction in Children with Obstructive Sleep Apnea. *Am J Respir Crit Care Med* 194, 1116–1126 (2016).
7. Khalyfa, A. *et al.* Effect on Intermittent Hypoxia on Plasma Exosomal Micro RNA Signature and Endothelial Function in Healthy Adults. *Sleep* 39, 2077–2090 (2016).
8. Khalyfa, A. *et al.* Plasma exosomes in OSA patients promote endothelial senescence: effect of long-term adherent continuous positive airway pressure. *Sleep* (2020) doi:10.1093/sleep/zsz217.
9. Marin, J. M. *et al.* Epigenetics modifications and Subclinical Atherosclerosis in Obstructive Sleep Apnea: The EPIOSA study. *BMC Pulm Med* 14, (2014).
10. Sanz-Rubio, D. *et al.* Stability of Circulating Exosomal miRNAs in Healthy Subjects article. *Sci Rep* (2018) doi:10.1038/s41598-018-28748-5.
11. Schrottmaier, W. C., Oskolkova, O. V., Schabbauer, G. & Afonyushkin, T. MicroRNA miR-320a modulates induction of HO-1, GCLM and OKL38 by oxidized phospholipids in endothelial cells. *Atherosclerosis* 235, 1–8 (2014).
12. Han, Q., Zhang, L. & Liao, R. Diagnostic and prognostic significance of miR-320a-3p in patients with chronic heart failure. *BMC Cardiovasc Disord* 24, (2024).
13. Chen, C. *et al.* MiR-320a contributes to atherogenesis by augmenting multiple risk factors and down-regulating SRF. *J Cell Mol Med* 19, 970–985 (2015).
14. Cortese, R. *et al.* Aorta macrophage inflammatory and epigenetic changes in a murine model of obstructive sleep apnea: Potential role of CD36. *Sci Rep* 7, (2017).
15. Badran, M. *et al.* Senolytic-facilitated Reversal of End-Organ Dysfunction in a Murine Model of Obstructive Sleep Apnea. *Am J Respir Crit Care Med* 209, 1001–1012 (2024).
16. Chen, B. *et al.* Exploring shared pathways and the shared biomarker ERRFI1 in Obstructive sleep apnoea and atherosclerosis using integrated bioinformatics analysis. *Sci Rep* 13, (2023).
17. Cortese, R., Sanz-Rubio, D., Kheirandish-Gozal, L., Marin, J. M. & Gozal, D. Epigenetic age acceleration in obstructive sleep apnoea is reversible with adherent treatment. *Eur Respir J* vol. 59 Preprint at <https://doi.org/10.1183/13993003.03042-2021> (2022).

18. Díaz-García, E. *et al.* PSGL-1: a novel immune checkpoint driving T-cell dysfunction in obstructive sleep apnea. *Front Immunol* 14, (2023).
19. Khalyfa, A., Gozal, D., Chan, W. C., Andrade, J. & Prasad, B. Circulating plasma exosomes in obstructive sleep apnoea and reverse dipping blood pressure. *Eur Respir J* 55, (2020).
20. Harki, O. *et al.* VE-cadherin cleavage in sleep apnoea: new insights into intermittent hypoxia-related endothelial permeability. *Eur Respir J* 58, (2021).

Journal Pre-proof

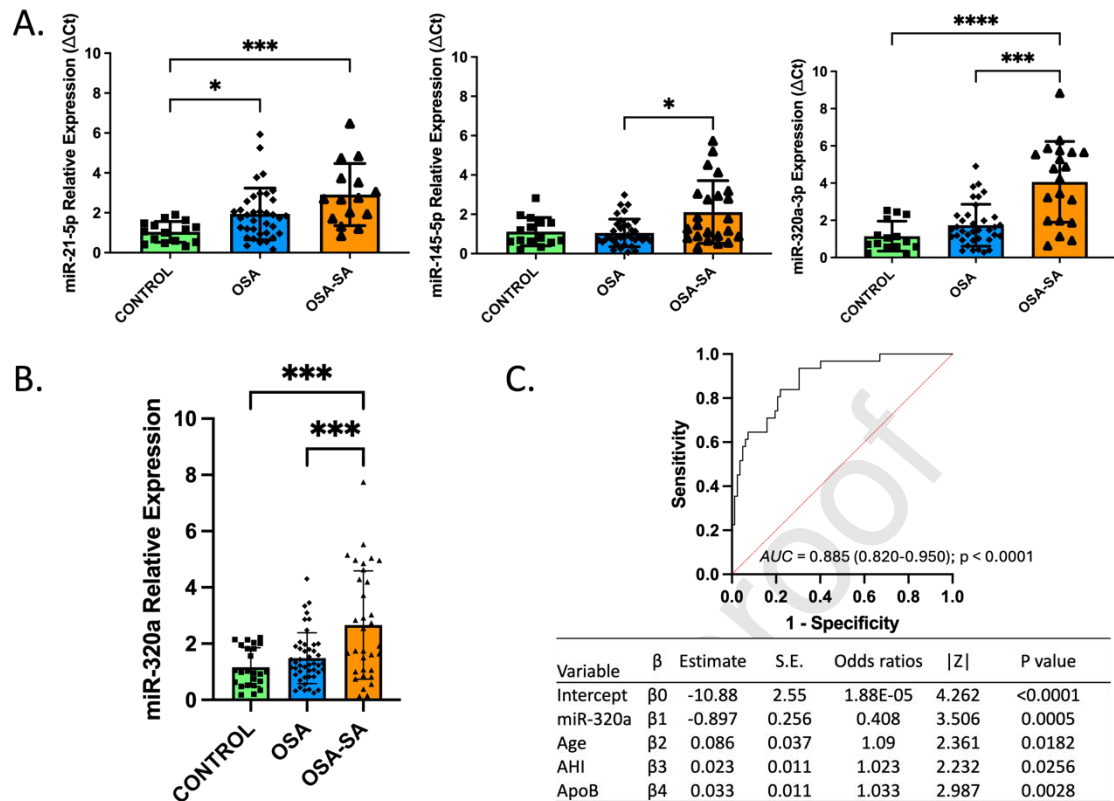


Figure 1. A) Relative expression of exosomal miRNAs exhibiting differential expression patterns in the derivation arm of the study. B) Validation of exosomal miR-320a-3p which showed increased relative expression in OSA-SA. C) Adjusted multivariable logistic regression model included miR-320a, age, AHI and ApoB for prediction of SA with a promising AUC value in the ROC curve analysis. OSA: Obstructive sleep apnea. OSA-SA: Overlap OSA and subclinical atherosclerosis. AHI: Apnea hypoapnea index. ApoB: apolipoprotein B. ROC: Receiver operating characteristic. AUC: Area under the curve. \*\*\*  $p < 0.001$ ; \*\*\*\*  $p < 0.0001$ .

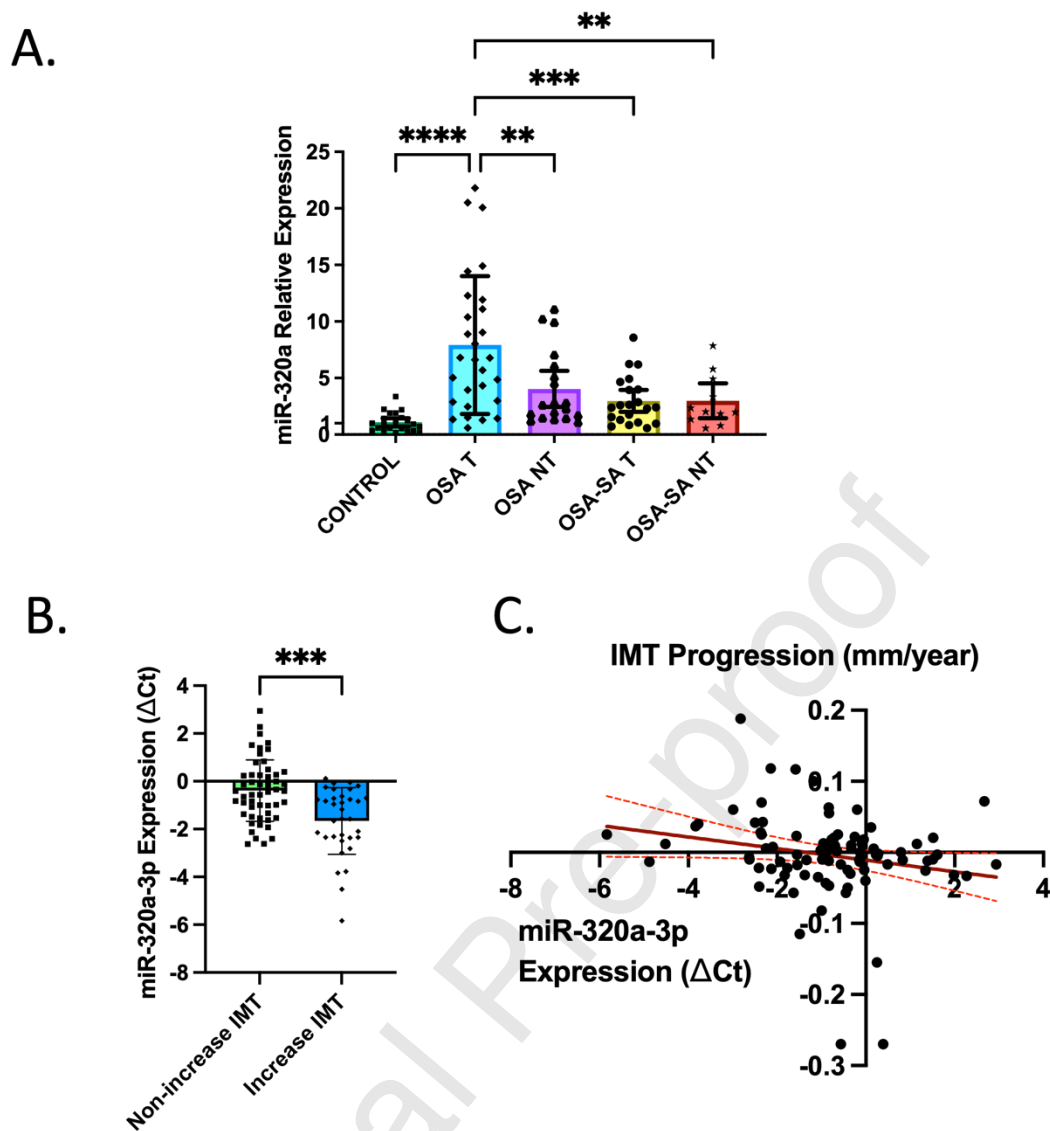


Figure 2. Progression of carotid intima media thickness (CIMT) and exosomal miR-320a-3p at 1-year follow-up. A) Relative expression of exosomal miR-320a-3p at 1-year follow-up. B) Delta Ct of exosomal miR-320a-3p in OSA at baseline classified according to their CIMT progression in the follow-up. C) Lineal regression between miR-320a-3p and IMT progression. OSA: Obstructive sleep apnea. OSA-SA: OSA and subclinical atherosclerosis. T: Treated with CPAP. NT: Not treated with CPAP. \*\*  $p < 0.01$ ; \*\*\*  $p < 0,001$ ; \*\*\*\*  $p < 0.0001$ .

# Circulating exosomal microRNAs and subclinical atherosclerosis in obstructive sleep apnea

## Supplementary material

### Supplementary Table 1. List of exosomal miRNAs analyzed in the derivation study.

miRNA	Selection
hsa-miR-16-5p	Candidate to normalization <sup>1</sup>
hsa-miR-21-5p	Atherosclerosis <sup>2</sup> and hypoxia <sup>3</sup>
hsa-miR-126-5p	Atherosclerosis <sup>4</sup>
hsa-miR-143-5p	Atherosclerosis <sup>5</sup>
hsa-miR-145-5p	Atherosclerosis <sup>6</sup>
hsa-miR-150-5p	Atherosclerosis <sup>7</sup> and inflammation <sup>8</sup>
hsa-miR-155-5p	Hypoxia <sup>9</sup>
hsa-miR-222-3p	Endothelial dysfunction <sup>10</sup> and hypoxia <sup>11</sup>
hsa-miR-223-3p	Cardiovascular diseases <sup>12</sup> and hypoxia <sup>13</sup>
hsa-miR-320a	Atherosclerosis <sup>14</sup>
hsa-let-7 g-5p	Atherosclerosis <sup>15</sup>
hsa-let-7a-5p	Candidate to normalization <sup>16</sup>

Supplementary Table 2. Clinical characteristics of subjects included in the derivation study.

Supplementary Table 3. Clinical characteristics of subjects included in the validation

	BASELINE VISIT		
	Control	OSA	OSA SA
Subjects, n	16	33	17
Sex (male, %)	81	81	82
Age (years)	47.8 ± 6.3	45.1 ± 9.3	51.9 ± 7.8 <sup>‡</sup>
BMI (kg/m <sup>2</sup> )	28.9 ± 3.6	30.3 ± 3.7	29.15 ± 4.31
SBP (mmHg)	119.7 ± 11.3	127.2 ± 13.6	136.2 ± 9.3 *
DBP (mmHg)	72.7 ± 7.8	82.1 ± 12.2 *	82.9 ± 10.7 *
AHI (events/hour)	2 ± 2	38.2 ± 20.5 *	44.5 ± 14.8 *
Nadir SaO <sub>2</sub>	84.8 ± 3.1	76.8 ± 8.7 *	75.4 ± 7.3 *
CT90, %	2.9 ± 6.5	17.6 ± 17 *	16.8 ± 16 *
ESS	10.6 ± 3.8	11.2 ± 5	8.5 ± 4.5
hsCRP (mg/dl)	0.24 ± 0.19	0.43 ± 0.41	0.31 ± 0.29
ApoA (mg/dl)	149.8 ± 24.8	147.5 ± 27.7	157.2 ± 29.8
ApoB (mg/dl)	103.7 ± 23.4	108.6 ± 30.3	122.8 ± 18.8
IMT (mm)	0.64 ± 0.1	0.67 ± 0.18	0.81 ± 0.2 *
Cho (mg/dl)	205.6 ± 37.5	207.4 ± 38.9	234.2 ± 36.7
HDL (mg/dl)	53.8 ± 15.4	49 ± 11.9	52.3 ± 12.5
LDL (mg/dl)	129 ± 27.7	126.3 ± 33.2	154.9 ± 33.8 <sup>‡</sup>
TG (mg/dl)	114.2 ± 41.3	150.1 ± 74.9	149.7 ± 71.8
CPAP use (mean hours per night)	-	-	-

AHI = Apnea-hypopnea index, BMI = body mass index, Cho = total cholesterol, hsCRP = high-sensitivity C-reactive protein (hsCRP), nadir SaO<sub>2</sub> = lowest oxygen saturation, CT90 = percentage of total sleep time with a percentage of O<sub>2</sub> saturation lower than 90%, %, DBP = diastolic blood pressure; ESS = Epworth sleepiness scale, HDL = high-density lipoprotein, IMT = intima-media thickness of the common carotid artery, LDL = low-density lipoprotein, SBP = systolic blood pressure, TG = triglycerides. All values are expressed as the mean ± standard deviation. Differences between controls and OSA groups: \*p-value < 0.05, \*\*p-value < 0.001, \*\*\*p-value < 0.001, Differences between SA and not SA: <sup>‡</sup>p-value < 0.05.

study.

BASELINE VISIT	FOLLOW-UP VISIT
----------------	-----------------

	Control	OSA	OSA SA	Control	OSA CPAP Treated	OSA Nontreated	OSA SA CPAP Treated	OSA SA Nontreated
Subjects, n	24	50	38	24	28	22	25	13
Sex (male, %)	75	76	79	75	75	77	82	76
Age (years)	44.3 ± 7.9	46.3 ± 8.7	47.3 ± 10.3	45.3 ± 8.1	46.5 ± 8.6	46 ± 7.9	48.1 ± 9.9	50 ± 11.8
BMI (kg/m <sup>2</sup> )	28.2 ± 3.9	31 ± 3.9	30.4 ± 5.6	28.4 ± 4.1	30.6 ± 4.5	29.8 ± 4.5	31.4 ± 5.4	26.9 ± 3.7
SBP (mmHg)	118.8 ± 12.6	128.8 ± 14.2*	133.6 ± 9.5*	117.1 ± 14.5	128.2 ± 13.7 *	128.1 ± 14.2 *	132.4 ± 12 *	124.7 ± 13.1
DBP (mmHg)	71.9 ± 9.3	81.9 ± 11.1*	83.5 ± 9.5*	71.1 ± 10.9	77.1 ± 8.5	80.2 ± 9.3	81 ± 8	74.9 ± 6.8
AHI (events/hour)	2 ± 1.3	43.2 ± 23.2 *	43.1 ± 21.6 *	3.4 ± 1.3	2.8 ± 1.8	18.3 ± 7.1 *, §	0.2 ± 0.1	16.6 ± 11.6 *, §
Nadir SaO <sub>2</sub>	86.1 ± 4	76 ± 7.9 *	74.2 ± 13.5 *	85.2 ± 4.7	82.2 ± 10.5	78.4 ± 9.5	87.4 ± 3.4	75.5 ± 13.7
CT90, %	2.6 ± 1	25 ± 21.1 *	15.5 ± 14.9 *	2.6 ± 1.6	4.7 ± 3	14.8 ± 12.6 *, §	1.1 ± 1	11.7 ± 9.7 *, §
ESS	10 ± 4	10.8 ± 4.9	9.5 ± 4.5	6.8 ± 4.5	7.9 ± 4.3	7.3 ± 3.9	5.3 ± 3.4	7.6 ± 5.9
hsCRP (mg/dl)	0.19 ± 0.17	0.42 ± 0.4 *	0.35 ± 0.28*	0.34 ± 0.3	0.36 ± 0.25	0.39 ± 0.3	0.42 ± 0.41	0.26 ± 0.2
ApoA (mg/dl)	149.6 ± 24	146.5 ± 28.4	153.1 ± 26.7	142.2 ± 45.6	140.5 ± 33.8	143.2 ± 37	141.5 ± 29.7	157.1 ± 22.3
ApoB (mg/dl)	100.1 ± 22.1	113.4 ± 34.5 *	118.3 ± 25.9 *	97.5 ± 24.1	114.1 ± 29.5	109.7 ± 29.7	108.2 ± 26.5	129.3 ± 33.7 *
IMT (mm)	0.59 ± 0.11	0.68 ± 0.2*	0.74 ± 0.18 **	0.61 ± 0.11	0.7 ± 0.19	0.65 ± 0.13	0.74 ± 0.19 *, ¥	0.79 ± 0.23 *, ¥
Cho (mg/dl)	202.8 ± 35.3	211.8 ± 39.6	223.1 ± 41.2	202 ± 27.5	213.9 ± 42	211 ± 33.1	205.7 ± 38.7	233.7 ± 32.6 *
HDL (mg/dl)	54.1 ± 14	48.5 ± 11.7	50.3 ± 11.5	53.5 ± 13.9	48 ± 13.6	49.2 ± 9.9	47.9 ± 10.9	56.4 ± 12.3
LDL (mg/dl)	126.6 ± 25.8	128.6 ± 34	144.2 ± 37.6	119.4 ± 32.9	128.3 ± 22.8	130.2 ± 31	130.6 ± 29.9	152.7 ± 18.3 *
TG (mg/dl)	110.3 ± 39.8	164 ± 85.9 *	150.3 ± 68.8 *	119.1 ± 51.1	152.6 ± 84.6	161.4 ± 86.7	136.4 ± 55.8	121.9 ± 82
CPAP use (mean h per night)	-	-	-	-	5.4 ± 1.1	-	5.5 ± 1.3	-

AHI = Apnea-hypopnea index, BMI = body mass index, Cho = total cholesterol, hsCRP = high-sensitivity C-reactive protein (hsCRP), nadir SaO<sub>2</sub> = lowest oxygen saturation, CT90 = percentage of total sleep time with a percentage of O<sub>2</sub> saturation lower than 90%, %, DBP = diastolic blood pressure; ESS = Epworth sleepiness scale, HDL = high-density lipoprotein, IMT = intima-media thickness of the common carotid artery, LDL = low-density lipoprotein, SBP = systolic blood pressure, TG = triglycerides. All values are expressed as the mean ± standard deviation. Differences between controls and OSA groups: \*p-value < 0.05, \*\*p-value < 0.001, \*\*\*p-value < 0.001, Differences between SA and not SA: ¥ p-value < 0.05. Differences between treated and not treated: § p-value < 0.05.

Figure S1. Characterization of exosomes. A) Images taken by transmission electron microscopy showing the presence of vesicles ranging from 50 to 100 nm. B) Representative profiles of Nanoparticle Tracking Assay. C) Dot blot confirming the presence of positive exosomal markers and absence of negative markers.

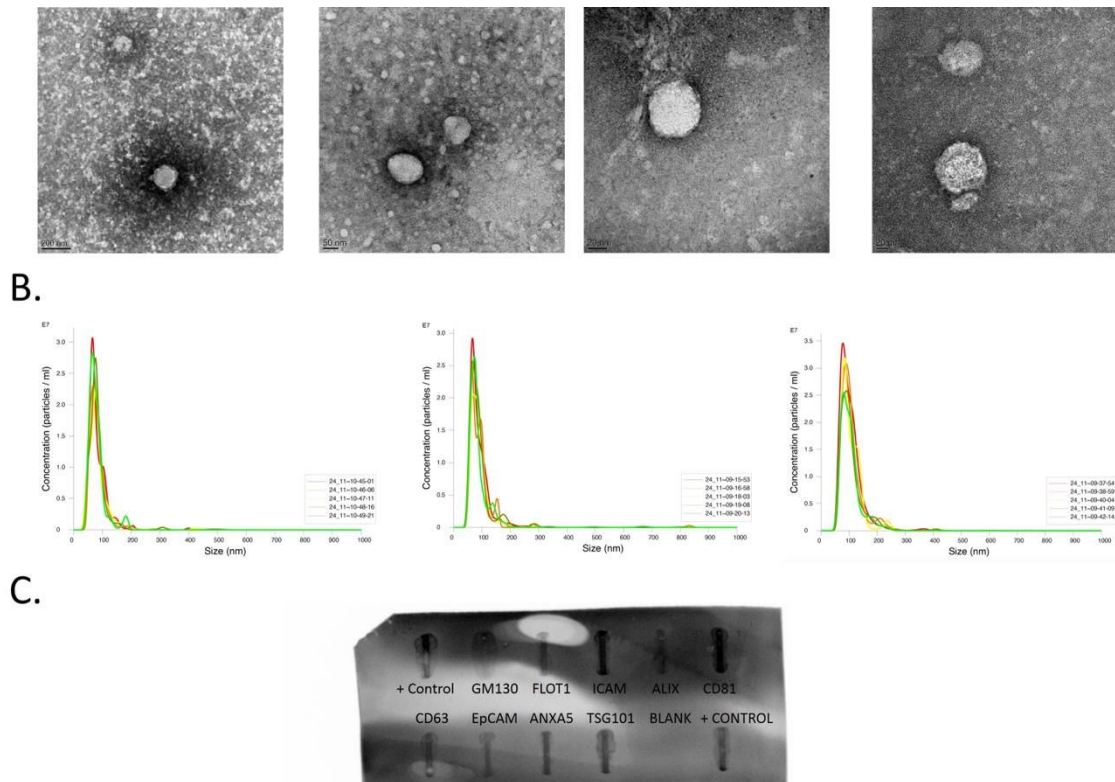
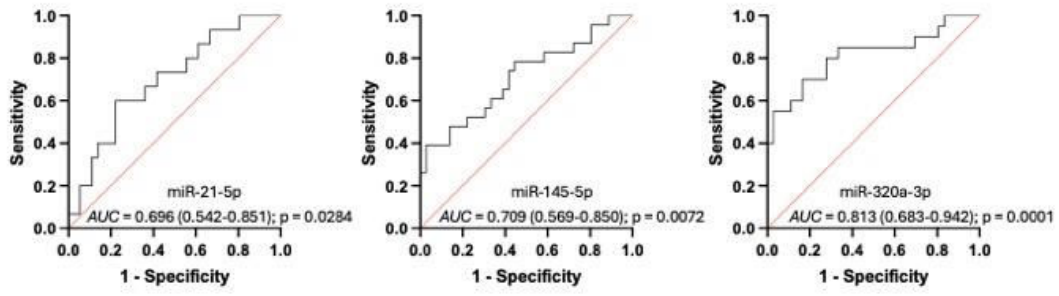
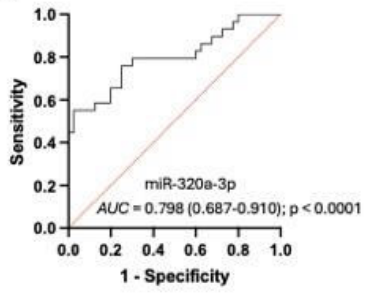


Figure S2. ROC curve analysis of univariate logistic models to predict subclinical atherosclerosis as outcome in the exploratory study (A) and the validation study (B).

A.



B.



Journal Pre-proof

Supplementary Table 4. Predicted targets of miR-320a.

Predicted Genes	RNF187 C12orf36 GCG ETFA TRIAP1 HECTD2 SMIM19 PCGF1 STARD4 NABP1 KITLG MLF1 RGS9BP RP1-127H14.3 RPA3-AS1 LPPR1 XAGE5 C1orf145 CD3G MBIP BLOC1S5 SDHD POLR1C ZFH3 HN1L GABRP KRTAP4-1 ASAH2C LILRB4 NXT2 PBX3 ST7-OT4 C6orf118 BX255923.1 C19orf40 DSCC1 CUTC CTSV FAM89A ARFIP1 ZWILCH ZNF214 ARPP19 MED7 KCNS3 CDCA3 DESI2 APEX1 YOD1 MYL12A MPPED2 YWHAH PCOLCE2 ARL8B AGFG1 RGS10 CGA RCN2 POU1F1 DAZAP1 ASAH2B GNAI1 RBM24 RBP7 DUSP16 DHX15 PCDHA5 PCDHA7 MRAP2 PCDHA12 PCDHA2 PCDHA10 PCDHA4 CDHA1 PCDHA6 PCDHA13 PCDHA11 PCDHA8 PCDHA3 PCDHA9 PCDHAC1 TMEM98 FBXO28 SYNGR2 CYP1A2 PAPD5 TFRC TMEM128 PCDHAC2 DPY30 TMEM47 MTRF1 CXorf38 ONECUT2 DLX1 RIOK3 ZNF23 ITGB1 C5orf51 MBL2 RAC1 CCSER2 CCR7 HHLA2 XAGE3 NIP7 COPS2 CDK6 KLHDC9 POLE3 DNER GAGE12B CCDC17 RP11-762I7.5 GSKIP RAD51AP1 CD160 SNTB1 CNKSR2 GTF2A1 10orf11 SLC46A2 POU2F1 GOLM1 LEF1 GTPBP8 HADH BCAP29 ZCCHC12 FAM154A TMEM254 OSTC TSC22D4 PAPOLA NAT1 ALOX12 MRPL35 MZT1 TGOLN2 AC004381.6 PFKM RAI2 MAGEB1 GRIK5 PRAMEF18 ACTL6A PRAMEF19 XAGE1C XAGE1B XAGE1D XAGE1E XAGE1A LEPR RBMXL1 SMNDC1 VDAC1 RP11-65D24.2 GAGE12J NKX2-4 UBE2C AP3M1 FADD GAGE13 RNASET2 UTP14C IQCA1 RASA1 GAGE10 TMEM255A GAGE2E GAGE2A SAMD5 MED21 GAGE12F GAGE12D GAGE12H GAGE12C GAGE12G HIST1H2BC PAGE1 METTL7A GAGE12E NKX3-1 TMEM230 ZRANB2 GAGE2D GAGE12I GAGE2C CD74 SLC10A7 SFTA3 FAM69B PPCS PNPO HTN1 MS12 ACTR2 ORM2 ORM1 MRPS18B
-----------------	--

Supplementary Table 5. GO Biological Process enrichment.

GO BIOLOGICAL PROCESS	GENES	PATHWAY GENES	ENRICHMENT FDR	GENES
GO:0007156 HOMOPHILIC CELL ADHESION VIA PLASMA MEMBRANE ADHESION MOLECULES	16	172	3.87E-04	PCDHA6 PCDHA9 PCDHA8 PCDHA7 PCDA5 PCDHA4 PCDHA2 PCDHA1 PCDHA13 PCDHAC2 PCDHAC1 PCDHA11 PCDHA10 PCDHA12 PCDHA3 ITGB1
GO:0098742 CELL-CELL ADHESION VIA PLASMA-MEMBRANE ADHESION MOLECULES	16	293	6.24E-07	PCDHA6 PCDHA9 PCDHA8 PCDHA7 PCDHA5 PCDHA4 PCDHA2 PCDHA1 PCDHA13 PCDHA2 PCDHAC1 PCDHA11 PCDHA10 PCDHA12 PCDHA3 ITGB1
GO:0098609 CELL-CELL ADHESION	28	1104	5.89E-08	MYL12A TMEM47 ACTL6A TFRC HHLA2 CD160 LEF1 ITGB1 CD74 KITLG PCDHA6 ALOX12 CCR7 FADD PCDHA9 PCDHA8 PCDHA7 PCDHA5 PCDHA4 PCDHA2 PCDHA1 PCDHA13 PCDHAC2 PCDHAC1 PCDHA11 PCDHA10 PCDHA12 PCDHA3
GO:0007155 CELL ADHESION	32	1729	0.000492	MYL12A PCDHA6 TMEM47 ITGB1 PCDHA9 PCDHA8 PCDHA7 PCDHA5 PCDHA4 PCDHA2 PCDHA1 PCDHA13 PCDHAC2 PCDHAC1 PCDHA11 PCDHA10PCDHA12 PCDHA3 CCR7 ACTL6A TFRC CDK6 HHLA2 CD160 LEF1 RASA1 CD74 KITLG ALOX12 ONECUT2 FADD ZFH3
GO:2000107 NEGATIVE REGULATION OF LEUKOCYTE APOPTOTIC PROCESS	5	58	0.0361	CCR7 CD74 KITLG SLC46A2 FADD
GO:0030217 T CELL DIFFERENTIATION	10	319	0.0545	CD3G ACTL6A TMEM98 CD74 CDK6 LEPR SLC46A2 CCR7 LEF1 FADD
GO:0021943 FORMATION OF RADIAL GLIAL SCAFFOLDS	2	3	0.0597	LEF1 ITGB1
GO:2000106 REGULATION OF LEUKOCYTE APOPTOTIC PROCESS	6	112	0.0597	CCR7 CD74 KITLG SLC46A2 FADD CD3G
GO:0042110 T CELL ACTIVATION	14	662	0.106	CD74 CD3G CCR7 ACTL6A TFRC HHLA2 CD160 TMEM98 KITLG CDK6 LEPR SLC46A2 LEF1 FADD

Supplementary Table 6. GO Molecular Function enrichment.

GO MOLECULAR FUNCTION	GENES	PATHWAY GENES	ENRICHMENT FDR	GENES
GO:0005509 CALCIUM ION BINDING	18	775	0.00660	RCN2 PCDHA6 MYL12A DNER PCDHA9 PCDHA8 PCDHA7 PCDHA5 PCDHA4 PCDHA2 PCDHA1 PCDHA13 PCDHAC2 PCDHAC1 PCDHA11 PCDHA10 PCDHA12 PCDHA3

Supplementary Table 7. PANTHER Pathway enrichment.

PATHWAY ENRICHMENT	GENES	PATHWAY GENES	ENRICHMENT FDR	GENES
P00012 CADHERIN SIGNALING PATHWAY	17	153	4,42E-07	ACTR2 LEF1 PCDHA1 PCDHA10 PCDHA11 PCDHA12 PCDHA13 PCDHA2 PCDHA3 PCDHA4 PCDHA5 PCDHA6 PCDHA7 PCDHA8 PCDHA9 PCDHAC1 PCDHAC2
P00057 WNT SIGNALING PATHWAY	16	292	8,12E-05	LEF1 PCDHA1 PCDHA10 PCDHA11 PCDHA12 PCDHA13 PCDHA2 PCDHA3 PCDHA4 PCDHA5 PCDHA6 PCDHA7 PCDHA8 PCDHA9 PCDHAC1 PCDHAC2

## Bibliography

1. Lange T, Stracke S, Rettig R, et al. Identification of miR-16 as an endogenous reference gene for the normalization of urinary exosomal miRNA expression data from CKD patients. Ray RB, ed. *PLoS One*. 2017;12(8):e0183435. doi:10.1371/journal.pone.0183435
2. Cengiz M, Yavuzer S, Kiliçkiran Avcı B, et al. Circulating miR-21 and eNOS in subclinical atherosclerosis in patients with hypertension. *Clin Exp Hypertens*. 2015;37(8):643-649. doi:10.3109/10641963.2015.1036064
3. Zuo K, Li M, Zhang X, et al. MiR-21 suppresses endothelial progenitor cell proliferation by activating the TGF $\beta$  signaling pathway via downregulation of WWP1. *Int J Clin Exp Pathol*. 2015;8(1):414-422. Accessed December 19, 2018. <http://www.ncbi.nlm.nih.gov/pubmed/25755729>
4. Schober A, Nazari-Jahantigh M, Wei Y, et al. MicroRNA-126-5p promotes endothelial proliferation and limits atherosclerosis by suppressing Dlk1. *Nat Med*. 2014;20(4):368-376. doi:10.1038/nm.3487
5. Xu R-H, Liu B, Wu J-D, Yan Y-Y, Wang J-N. miR-143 is involved in endothelial cell dysfunction through suppression of glycolysis and correlated with atherosclerotic plaques formation. *Eur Rev Med Pharmacol Sci*. 2016;20(19):4063-4071. Accessed December 19, 2018. <http://www.ncbi.nlm.nih.gov/pubmed/27775792>
6. Sala F, Aranda JF, Rotllan N, et al. MiR-143/145 deficiency attenuates the progression of atherosclerosis in Ldlr $^{-/-}$  mice. *Thromb Haemost*. 2014;112(4):796-802. doi:10.1160/TH13-11-0905
7. Li J, Zhang S. microRNA-150 inhibits the formation of macrophage foam cells through targeting adiponectin receptor 2. *Biochem Biophys Res Commun*. 2016;476(4):218-224. doi:10.1016/j.bbrc.2016.05.096
8. Chen M, Shen C, Zhang Y, Shu H. MicroRNA-150 attenuates hypoxia-induced excessive proliferation and migration of pulmonary arterial smooth muscle cells through reducing HIF-1 $\alpha$  expression. *Biomed Pharmacother*. 2017;93:861-868. doi:10.1016/j.biopha.2017.07.028
9. Yang D, Wang J, Xiao M, Zhou T, Shi X. Role of Mir-155 in Controlling HIF-1 $\alpha$  Level and Promoting Endothelial Cell Maturation. *Sci Rep*. 2016;6(1):35316. doi:10.1038/srep35316
10. Xue Y, Wei Z, Ding H, et al. MicroRNA-19b/221/222 induces endothelial cell dysfunction via suppression of PGC-1 $\alpha$  in the progression of atherosclerosis. *Atherosclerosis*. 2015;241(2):671-681. doi:10.1016/j.atherosclerosis.2015.06.031
11. Camps C, Saini HK, Mole DR, et al. Integrated analysis of microRNA and mRNA expression and association with HIF binding reveals the complexity of microRNA expression regulation under hypoxia. *Mol Cancer*. 2014;13(1):28. doi:10.1186/1476-4598-13-28
12. Dai G-H, Ma P-Z, Song X-B, Liu N, Zhang T, Wu B. MicroRNA-223-3p Inhibits the Angiogenesis of Ischemic Cardiac Microvascular Endothelial Cells via Affecting RPS6KB1/hif-1 $\alpha$  Signal Pathway. Ahrens I, ed. *PLoS One*. 2014;9(10):e108468. doi:10.1371/journal.pone.0108468

13. Zeng Y, Zhang X, Kang K, et al. MicroRNA-223 Attenuates Hypoxia-induced Vascular Remodeling by Targeting RhoB/MLC2 in Pulmonary Arterial Smooth Muscle Cells. *Sci Rep*. 2016;6(1):24900. doi:10.1038/srep24900
14. Chen C, Wang Y, Yang S, et al. MiR-320a contributes to atherogenesis by augmenting multiple risk factors and down-regulating SRF. *J Cell Mol Med*. 2015;19(5):970-985. doi:10.1111/jcmm.12483
15. Wang Y-S, Hsi E, Cheng H-Y, Hsu S-H, Liao Y-C, Juo S-HH. Let-7g suppresses both canonical and non-canonical NF- $\kappa$ B pathways in macrophages leading to anti-atherosclerosis. *Oncotarget*. 2017;8(60):101026-101041. doi:10.18632/oncotarget.18197
16. Stamova BS, Apperson M, Walker WL, et al. Identification and validation of suitable endogenous reference genes for gene expression studies in human peripheral blood. *BMC Med Genomics*. 2009;2(1):49. doi:10.1186/1755-8794-2-49

Journal Pre-proof